STRAIN LOCALIZATION ANALYSIS USING A LARGE STRAIN SELF-CONSISTENT APPROACH

G.Franz[1], F.Abed-Meraim[1], T.Ben Zineb[2], X.Lemoine[3], M.Berveiller[1]

1 : LPMM CNRS UMR 7554 ENSAM CER de Metz, 4 rue Augustin Fresnel 57078 Metz Cedex 3

2 : LEMTA CNRS UMR 7563 ESSTIN - UHP, 2 Rue Jean Lamour 54519 Vandoeuvre-Lès-Nancy

3 : Centre Automobile Produit ARCELOR Research, S.A. Voie Romaine BP 30320 57283 Maizières-les-Metz

Context of the study

Mechanisms of ductility loss

Plastic mechanisms of ductility loss

Structural origin: wrinkling, buckling

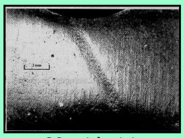

Material origin: localization, necking

Damage mechanisms of ductility loss

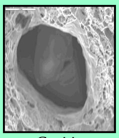

Cavitie

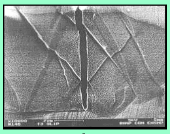

Failure

Forming Limit Diagram (FLD)

- Forming limit of sheet metal = state at which a localized strain initiates during forming
- Ductility loss characterization using Forming Limit Diagram (FLD) developed first by Keeler (1963) and Goodwin (1968).
- Path-dependent representation

Metallurgy impact (texture, grain size, …)

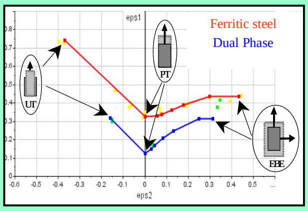

Strain path dependence

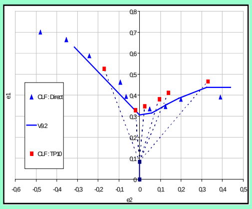

Plastic anisotropy evolution

Plastic anisotropy evolution

Textural anisotropy (crystalographic network + morphology)	Structural anisotropy (intragranular microstructure)

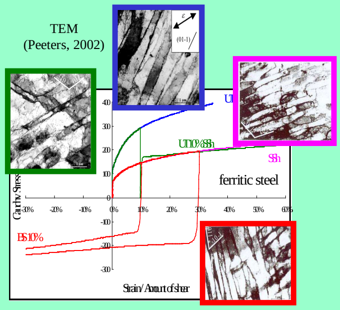

Aims of the study

- Ductility loss prediction for monotonous and sequential strain paths
- Optimization of microstructural properties for the sheet forming steels

Take metallurgy, mechanisms, microstructure and textures into account

Scales transitions tools, micromechanic of plasticity, localization and damage criteria, coupling with finites elements

Steel behaviour during sheet forming: hardening, complex loads, instabilities, anisotropy

- Three main step :
  - Single crystal modeling,
  - Scale transition,
  - Ductility loss criterion

Single crystal modeling

Mesoscopic scale – basic slip process

Assumptions

- Elastic-plastic behavior
- Large strains formulation
- Body-Centered Cubic (BCC)
- Plastic strains only due to slip processes (<110> slip direction family and {110}, {112} slip plane families)

Elasticity $\hat{\sigma} = C : (d - d^p) - \sigma \, trace(d)$

Plasticity

$$\dot{\tau}^g = \hat{\sigma} : R^g \qquad d^p = R^g \dot{\gamma}^g \qquad w^p = S^g \dot{\gamma}^g$$

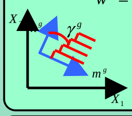

Elastic-plastic tangent modulus

$$\dot{n} = l : g$$

$$l_{ijkl} = \left[C_{ijkl} - \frac{1}{2}(\delta_{ik}\sigma_{lj} + \delta_{il}\sigma_{kj}) - \frac{1}{2}(\sigma_{ik}\delta_{lj} - \sigma_{il}\delta_{jk}) \right] - \left[C_{ijpq} R^g_{pq} + S^g_{ip}\sigma_{pj} - \sigma_{ip} S^g_{pj} \right] M_{gh} k^h R^h_{mn} (C_{mnkl} - \sigma_{mn}\delta_{kl})$$

$$\text{with } M^{gh} = \left(\delta^{gh} + k^g R^g_{ij} C_{ijkl} R^h_{kl} \right)^{-1}$$

Microscopic scale – intragranular microstructure

- The statistically stored dislocations in the cell interior, as well as the cell boundary dislocations, are represented by a single local dislocation density ρ
- The local density of immobile dislocations stored in the wall $\rho^{(wd)}$ associated with the {110} plane
- The polarity dislocations density $\rho^{(wp)}$ associated with the {110} plane

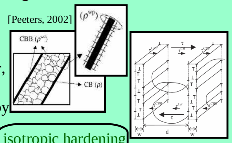

Mughrabi's composite model

isotropic hardening $\tau^{CB} = \alpha\mu b\sqrt{\rho}$

$$\tau^g_c = \tau_0 + (1-f)\tau^{CB} + f\sum_{i=1}^{6}\tau^{CBB}_{ig}$$

latent hardening

$$\tau^{wd}_{ig} = \alpha\mu b\sqrt{\rho^{wd}_i}\, abs(m_g.n^w_i)$$

polarity

$$\tau^{wp}_{ig} = \alpha\mu b \left\langle \sqrt{abs(\rho^{wp}_i)}\, m_g.n^w_i \, sign(\rho^{wp}_i) \right\rangle$$

Scale transition

What is the link between local and global strain?

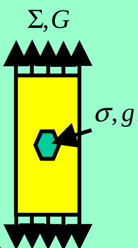

Volumic average

$$\dot{N}_{ij} = \frac{1}{V}\int_V \dot{n}_{ij}\, dV \qquad G_{ij} = \frac{1}{V}\int_V g_{ij}\, dV$$

Fourth order localization tensors

$$\dot{n}_{ij} = B_{ijkl}\dot{N}_{kl} \qquad g_{ij} = A_{ijkl} G_{kl} \qquad L^{eff}_{ijkl} = \overline{l_{ijmn} A_{mnkl}}$$

Relation between A and B

$$A_{jkl} = l^{-1}_{ijmn} B_{mnpq} L^{eff}_{pqkl}$$

Ductility loss criterion

Assumption: the onset of localization is along a band (Rice,1976)

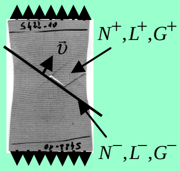

Field equations

$$\begin{cases} div(\dot{N}^T) = 0 \\ G = grad(V) \\ \dot{N} = L : G \\ \text{Boundary conditions} \end{cases}$$

Ellipticity loss

$$\det(\boldsymbol{v}.\boldsymbol{L}.\boldsymbol{v}) = 0$$

Microscopic validation

TEM micrograph

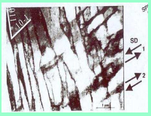

Longitudinal plane view TEM micrograph in a grain with initial orientation (43.3°,127.8°,-42.4°) after a reverse test of 30% simple shear with SD parallel RD and SPN parallel to TD [Nesterova & al, 2001]

Intensity of dislocations walls

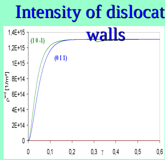

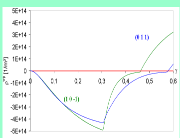

Polarity of dislocations walls

Macroscopic validation

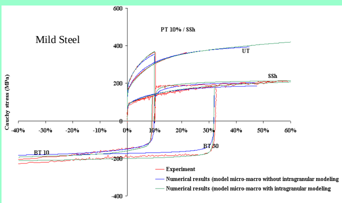

Forming Limit Diagrams

Direct FLD

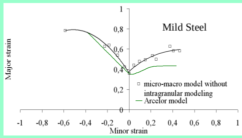

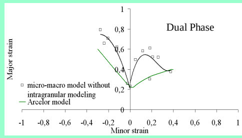

- The positive side of the FLD is overestimated. This effect can be corrected by damage introduction in the model

Complex FLD: Equibiaxial Expansion prestrain (10%)

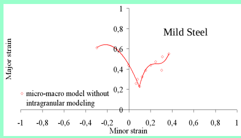

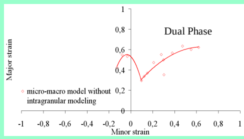

- The level of FLD after expansion prestrain seems to be realistic. The curve is shifted down and at the right in agreement with tendancies observed in literature

Complex FLD: Uniaxial Tension prestrain (10%)

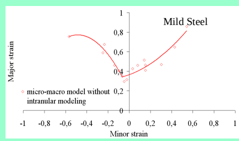

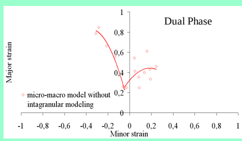

- FLD is shifted at the left in agreement with tendancies observed in literature but the level of the lower point of the FLD is lower

Conclusions

Multiscale model with intraganular modeling

- Reproduces correctly the intragranular microstructure during monotonic and sequential loading paths
- Gives better results concerning macroscopic behavior during changing loading paths than model without intragranular modeling

Multiscale model without intraganular modeling

- Reproduces correctly the shape and the level of direct FLD for mild steel and dual phase
- Reproduces the strain-path dependence of complex FLD